

# Static and Dynamic Fusion for Multi-modal Cross-ethnicity Face Anti-spoofing

Ajian Liu<sup>1\*</sup>, Zichang Tan<sup>2\*</sup>, Xuan Li<sup>3</sup>, Jun Wan<sup>2†</sup>, Sergio Escalera<sup>4</sup>, Guodong Guo<sup>5</sup>, Stan Z. Li<sup>1,2</sup>

<sup>1</sup>MUST, Macau, China; <sup>2</sup>NLPR, CASIA, China; <sup>3</sup>BJTU, China; <sup>4</sup>CVC, UB, Spain; <sup>5</sup>Baidu Research, China  
 {jun.wan, szli}@ia.ac.cn, sergio@maia.ub.es, guogudong01@baidu.com

## Abstract

Regardless of the usage of deep learning and hand-crafted methods, the dynamic information from videos and the effect of cross-ethnicity are rarely considered in face anti-spoofing. In this work, we propose a static-dynamic fusion mechanism for multi-modal face anti-spoofing. Inspired by motion divergences between real and fake faces, we incorporate the dynamic image calculated by rank pooling with static information into a conventional neural network (CNN) for each modality (i.e., RGB, Depth and infrared (IR)). Then, we develop a partially shared fusion method to learn complementary information from multiple modalities. Furthermore, in order to study the generalization capability of the proposal in terms of cross-ethnicity attacks and unknown spoofs, we introduce the largest public cross-ethnicity Face Anti-spoofing (CASIA-CeFA) dataset, covering 3 ethnicities, 3 modalities, 1607 subjects, and 2D plus 3D attack types. Experiments demonstrate that the proposed method achieves state-of-the-art results on CASIA-CeFA, CASIA-SURF, OULU-NPU and SiW.

## 1. Introduction

In order to enhance security of face recognition systems, the presentation attack detection (PAD) technique is a vital stage prior to visual face recognition [4, 5, 20, 28]. Most works in face anti-spoofing focus on still-images, including RGB, Depth or IR. These methods can be divided into two main categories: handcrafted methods [4, 10, 27] and deep learning based methods [12, 19, 26]. Handcrafted methods attempt to extract texture information or statistical features (i.e., HOG [18, 36] and LBP [22, 10]) to distinguish between real and spoof faces. Deep learning based methods automatically learn discriminative features from input images for face anti-spoofings [19, 26]. However, the analysis

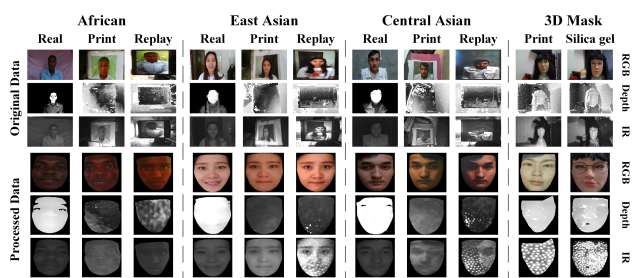


Figure 1. Samples of the CASIA-CeFA dataset. It contains 1607 subjects, 3 different ethnicities (i.e., Africa, East Asia, and Central Asia), with 4 attack types (i.e., print attack, replay attack, 3D print and silica gel attacks).

of motion divergences between real and fake faces received little attention. In order to improve robustness in real applications, some temporal-based methods [24, 26] have been proposed, which require from a constrained human guided interaction, such as movements of eyes, lips, and head. However, this does not provide with a natural user friendly interaction. Different from those works, we capture the temporal/dynamic information by using dynamic image generated by rank pooling [14], which doesn't need any human guide interaction. Moreover, inspired by the motion divergences between real and fake faces, a static- and dynamic-based network (SD-Net) is further formulated by taking the static and dynamic images as the input.

Multi-modal face anti-spoofing have also absorbed an increasing number of researchers in recent two years. Some fusion methods [41, 25] are published, which restrict the interactions among different modalities since they are independent before the fusion. But it is difficult for different modalities to effectively utilize the modality relatedness from the beginning of the network to its end to boost the overall performance. In this paper, we propose a partially shared branch multi-modal network (PSMM-Net) with allowing the exchanges and interactions among dif-

\*Equal Contribution

†Corresponding Author, email: jun.wan@ia.ac.cn

ferent modalities, aiming to capture correlated and complementary features.

Dataset	Year	# sub	# num	Attacks	Mod.	Dev.	Eth.
Replay-Attack [7]	2012	50	1200	Pr,Re	R	CR	*
CASIA-FASD [42]	2012	50	600	Pr,Cu,Re	R	CR	*
3DMAD [11]	2014	17	255	M	R/D	CR/K	*
MSU-MFSD [35]	2015	35	440	Pr,Re	R	P/L	*
Replay-Mobile [9]	2016	40	1030	Pr,Re	R	P	*
Msspoof [8]	2016	21	4704 <sup>a</sup>	Pr	R/I	CR/CI	*
OULU-NPU [6]	2017	55	5940	Pr,Re	R	CR	*
SiW [20]	2018	165	4620	Pr,Re	R	CR	AS/A/ U/I
CASIA-SURF [41]	2019	1000	21000	Pr,Cu	R/D/I	S	E
CASIA-CeFA(Ours)	2019	1500	18000	Pr, Re	R/D/I	S	A/E/C
		99	5346	M			
		8	192	G			
		Total: 1607 subjects, 23538 videos					

Table 1. Comparisons among existing face PAD databases. (*i* and *\** indicates the dataset only contains images and does not provide specific ethnicities, respectively. Mod.: modalities, Dev.: devices, Eth.: ethnicities, Pr: print attack, Re: replay attack, Cu: Cut, M: 3D print face mask, G: 3D silica gel face mask, R: RGB, D: Depth, I: IR, CR: RGB Camera, CI: IR Camera, K: Kinect, P: Cellphone, L: Laptop, S: Intel Realsense, AS: Asian, A: Africa, U: Caucasian, I: Indian, E: East Asia, C: Central Asia.)

Furthermore, data plays a key role in face anti-spoofing tasks. About existing face anti-spoofing datasets, such as CASIA-FASD [42], Replay-Attack [7], OULU-NPU [6], and SiW [20], the amount of sample is relatively small and most of them just contain the RGB modality. The recently released CASIA-SURF [41] includes 1,000 subjects and RGB, Depth and IR modalities. Although this provides with a larger dataset in comparison to the existing alternatives, it suffers from limited attack types (2D print attack) and single ethnicity (Chinese people). Overall, the effect of cross-ethnicity for face anti-spoofing received little attention in previous works. Therefore, we introduce CASIA-CeFA dataset, the largest dataset in terms of subjects (see Table 1). In CASIA-CeFA, attack types are diverse, including printing from cloth, video replay attack, 3D print and silica gel attacks. More importantly, it is the first public dataset designed for exploring the impact of cross-ethnicity in the study of face anti-spoofing. Some samples of the CASIA-CeFA dataset are shown in Fig. 1.

To sum up, the contributions of this paper are summarized as follows: (1) We propose the SD-Net to learn both static and dynamic features for single modality. It is the first work incorporating dynamic images for face anti-spoofing. (2) We propose the PSMM-Net to learn complementary information from multi-modal data in videos. (3) We release the CASIA-CeFA dataset, which includes 3 ethnicities, 1607 subjects and 4 diverse 2D/3D attack types. (4) Extensive experiments of the proposed method on CASIA-CeFA and other 3 public datasets verify its high generalization capability.

## 2. Related Work

### 2.1. Methods

**Image-based Methods.** Image-based methods take still images as input, *i.e.*, RGB, Depth or IR. Classical approaches based on handcrafted features, such as HOG [36], LBP [22, 10], SIFT [27] or SURF [4] together with traditional classifiers, such as SVM or LDA, to perform binary anti-spoofing predictions. However, those methods lack of good generalization capability when testing conditions vary, such as lighting and background. Owing to the success of deep learning strategies over handcrafted alternatives in computer vision, some works [12, 19, 26] extended feature vectors with features from CNN networks for face anti-spoofing. Authors of [3, 20] presented a two-stream network using RGB and Depth images as input. The work of [21] proposes a deep tree network to model spoofs by hierarchically learning sub-groups of features. However, previous methods do not consider any kind of temporal information for face anti-spoofing.

**Temporal-based Methods.** In order to improve robustness in real applications, some temporal-based methods [24, 26] have been proposed, which require from a constrained human guided interaction, such as movements of eyes, lips, and head. However, those methods do not provide with a natural user friendly interaction. Even more importantly, these methods [24, 26] could become vulnerable if someone presents a replay attack or a print photo attack with cut eye/mouth regions. Given that the Photoplethysmography (rPPG) signals (*i.e.* heart plus signal) can be detected from real but not spoof, Liu *et al.* [20] proposed a CNN-RNN model to estimate rPPG signals with sequence-wise supervision and face depth with pixel-wise supervision. The estimated depth and rPPG are fused to distinguish real and fake faces. Feng *et al.* [12] distinguished between real and fake samples based on the the difference between image quality and optical flow information. Yang *et al.* [37] proposed a spatio-temporal attention mechanism to fuse global temporal and local spatial information. All previous methods rely on a single visual modality, and no work considers the effect of cross-ethnicity for anti-spoofing.

**Multi-modal Fusion Methods.** Zhang *et al.* [41] proposed a fusion network with 3 streams using ResNet-18 as the backbone, where each stream is used to extract low level features from RGB, Depth and IR data, respectively. Then, these features are concatenated and passed to the last two residual blocks. Similar to [41], Aleksandr *et al.* [25] used a fusion network with 3 streams. They used ResNet-34 as the backbone and multi-scale feature fusion at all residual blocks. Tao *et al.* [29] proposed a multi-stream CNN architecture called FaceBagNet, which uses patch-level images as input and modality feature erasing (MFE) operation to prevent overfitting and obtain more discriminative fused

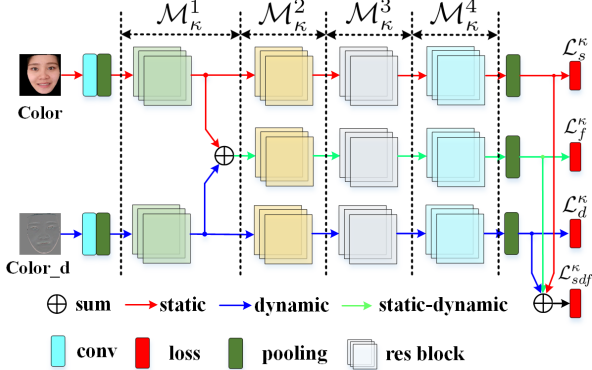


Figure 2. SD-Net diagram, showing a single-modal static-dynamic-based network. We take the RGB modality and its corresponding dynamic image as an example. This architecture includes three branches: static (red arrow), dynamic (blue arrow) and static-dynamic (green arrow). The static-dynamic branch fuses the static and dynamic features of first res block outputs from static and dynamic branches (best viewed in color).

features. All previous methods just consider as a key fusion component the concatenation of features from multiple modalities. Unlike [41, 25, 29], we propose the PSM-Net, where three modality-specific networks and one shared network are connected by using a partially shared structure to learn discriminative fused features for face anti-spoofing.

## 2.2. Datasets

Table 1 lists existing face anti-spoofing datasets. One can see that before 2019 the maximum number of available subjects was 165 on the SiW dataset [20]. That was clearly limiting the generalization ability of new approaches for cross-dataset evaluation. Most of the datasets just contain RGB data, such as Replay-Attack [7], CASIA-FASD [42], SiW [20] and OULU-NPU [6]. Recently, the CASIA-SURF [41] has been released, including 1000 subjects with three modalities, namely RGB, Depth and IR. Although this relieved the problem of the amount of data, it is limited in terms of attack types (only 2D print attack) and only includes 1 ethnicity (Chinese people). As shown in Table 1, most datasets do not provide ethnicity information, except SiW and CASIA-SURF. Although the SiW dataset provides four ethnicities, it still does not consider the effect of cross-ethnicity for face anti-spoofing. This limitation also holds for the CASIA-SURF dataset.

## 3. Proposed Method

### 3.1. SD-Net for Single-modal

**Single-modal Dynamic Image Construction.** Rank pooling [14, 33] defines a rank function that encodes a video into a feature vector. The learning process can be seen as a convex optimization problem using the RankSVM [30] for-

mulation in Eq.1. Let RGB (Depth or IR) video sequence with  $K$  frames be represented as  $\langle \mathbf{I}_1, \mathbf{I}_2, \dots, \mathbf{I}_i, \dots, \mathbf{I}_K \rangle$ , and  $\mathbf{I}_i$  denotes the average of RGB (Depth or IR) features over time up to  $i$ -frame. The process is formulated below.

$$\begin{aligned} \underset{\mathbf{d}}{\operatorname{argmin}} \quad & \frac{1}{2} \|\mathbf{d}\|^2 + \delta \times \sum_{i>j} \xi_{ij} \\ \text{s.t.} \quad & \mathbf{d}^T \cdot (\mathbf{I}_i - \mathbf{I}_j) \geq 1 - \xi_{ij}, \xi_{ij} \geq 0 \end{aligned} \quad (1)$$

where  $\xi_{ij}$  is the slack variable, and  $\delta = \frac{2}{K(K-1)}$ .

By optimizing Eq. 1, we map a sequence of  $K$  frames to a single vector  $\mathbf{d}$ . In this paper, rank pooling is directly applied on the pixels of RGB (Depth or IR) frames and the dynamic image  $\mathbf{d}$  is of the same size as the input frames. In our case, given input frame, we compute its dynamic image online with rank pooling using  $K$  consecutive frames. Our selection of dynamic images for rank pooling in SD-Net is further motivated by the fact that dynamic images have proved its superiority to regular optical flow [32, 14].

**Single-modal SD-Net.** As shown in Fig. 2, taking the RGB modality as an example, we propose the SD-Net to learn hybrid features from static and dynamic images. It contains 3 branches: static, dynamic and static-dynamic branches, which learn complementary features. The network takes ResNet-18 [16] as the backbone. For static and dynamic branches, each of them consists of 5 blocks (*i.e.*, conv, res1, res2, res3, res4) and 1 Global Average Pooling (GAP) layer, while in the static-dynamic branch, the conv and res1 blocks are removed because it takes fused features of res1 blocks from static and dynamic branches as input.

For convenience of terminology with the rest of the paper, we divide residual blocks of the network into a set of modules  $\{\mathcal{M}_\kappa^t\}_{t=1}^4$  according to feature level, where  $\kappa \in \{color, depth, ir\}$  is an indicator of the modality and  $t$  represents the feature level. Except for the first module  $\mathcal{M}_\kappa^1$ , each module extracts static, dynamic and static-dynamic features by using a residual block, denoted as  $\mathbf{X}_{s,\kappa}^t$ ,  $\mathbf{X}_{d,\kappa}^t$  and  $\mathbf{X}_{f,\kappa}^t$ , respectively. The output features from each module are used as the input for the next module. The static-dynamic features  $\mathbf{X}_{f,\kappa}^1$  of the first module are obtained by directly summing  $\mathbf{X}_{s,\kappa}^1$  and  $\mathbf{X}_{d,\kappa}^1$ .

In order to ensure each branch learns independent features, each branch employs an independent loss function after the GAP layer [31]. In addition, a loss function based on the summed features from all three branches is employed. The binary cross-entropy loss is used as the loss function. All branches are jointly and concurrently optimized to capture discriminative and complementary features for face anti-spoofing in image sequences. The overall objective function of SD-Net for the  $\kappa^{th}$  modality is defined as:

$$\mathcal{L}^\kappa = \mathcal{L}_s^\kappa + \mathcal{L}_d^\kappa + \mathcal{L}_f^\kappa + \mathcal{L}_{sdf}^\kappa \quad (2)$$

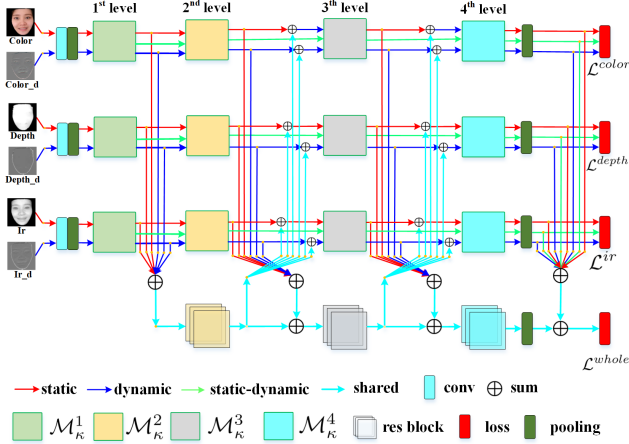


Figure 3. The PSMM-Net diagram. It consists of two main parts. The first is the modality-specific network, which contains three SD-Nets to learn features from RGB, Depth, IR modalities, respectively. The second is a shared branch for all modalities, which aims to learn the complementary features among different modalities.

where  $\mathcal{L}_s^\kappa$ ,  $\mathcal{L}_d^\kappa$ ,  $\mathcal{L}_f^\kappa$  and  $\mathcal{L}_{sdf}^\kappa$  are the losses for static branch, dynamic branch, static-dynamic branch, and summed features from all three branches of the network, respectively.

### 3.2. PSMM-Net for Multi-modal Fusion

The architecture of the proposed PSMM-Net is shown in Fig. 3. It consists of two main parts: a) the modality-specific network, which contains three SD-Nets to learn features from RGB, Depth, IR modalities, respectively; b) and a shared branch for all modalities, which aims to learn the complementary features among different modalities.

For the shared branch, we adopt ResNet-18, removing the first conv layer and res1 block. In order to capture correlations and complementary semantics among different modalities, information exchange and interaction among SD-Nets and the shared branch are designed. This is done in two different ways: a) forward feeding of fused SD-Net features to the shared branch, and b) backward feeding from shared branch modules output to SD-Net block inputs.

**Forward Feeding.** We fuse static and dynamic SD-Nets features from all modality branches and fed them as input to its corresponding shared block. The fused process at  $t^{th}$  feature level can be formulated as:

$$\tilde{\mathbf{S}}^t = \sum_{\kappa} \mathbf{X}_{s,\kappa}^t + \sum_{\kappa} \mathbf{X}_{d,\kappa}^t + \mathbf{S}^t \quad t = 1, 2, 3 \quad (3)$$

In the shared branch,  $\tilde{\mathbf{S}}^t$  denotes the input to the  $(t+1)^{th}$  block, and  $\mathbf{S}^t$  denotes the output of the  $t^{th}$  block. Note that the first residual block is removed from the shared branch, thus  $\mathbf{S}^1$  equals to zero.

**Backward Feeding.** Shared features  $\mathbf{S}^t$  are delivered back to the SD-Nets of the different modalities. The static

features  $\mathbf{X}_{s,\kappa}^t$  and dynamic features  $\mathbf{X}_{d,\kappa}^t$  add with  $\mathbf{S}^t$  for feature fusion. This can be denoted as:

$$\tilde{\mathbf{X}}_{s,\kappa}^t = \mathbf{X}_{s,\kappa}^t + \mathbf{S}^t, \quad \tilde{\mathbf{X}}_{d,\kappa}^t = \mathbf{X}_{d,\kappa}^t + \mathbf{S}^t \quad (4)$$

where  $t$  ranges from 2 to 3.

After feature fusion,  $\tilde{\mathbf{X}}_{s,\kappa}^t$  and  $\tilde{\mathbf{X}}_{d,\kappa}^t$  become the new static and dynamic features, which are then feed to the next module  $\mathcal{M}_{\kappa}^{t+1}$ . Note that the exchange and interaction among SD-Nets and the shared branch are only performed for static and dynamic features. This is done to avoid hybrid features among static and dynamic information to be disturbed by multi-modal semantics.

**Loss Optimization.** There are two main kind of losses employed to guide the training of PSMM-Net. The first corresponds to the losses of the three SD-Nets, *i.e.*, color and depth and ir modalities, denoted as  $\mathcal{L}^{color}$ ,  $\mathcal{L}^{depth}$  and  $\mathcal{L}^{ir}$ , respectively. The second corresponds to the loss that guides the entire network training, denoted as  $\mathcal{L}^{whole}$ , which bases on the summed features from all SD-Nets and the shared branch. The overall loss  $\mathcal{L}$  of PSMM-Net is denoted as:

$$\mathcal{L} = \mathcal{L}^{whole} + \mathcal{L}^{color} + \mathcal{L}^{depth} + \mathcal{L}^{ir} \quad (5)$$

## 4. CASIA-CeFA dataset

This section describes the CASIA-CeFA dataset. The motivation of this dataset is to provide with an increased diversity of attack types compared to existing datasets, as well as to explore the effect of cross-ethnicity in face anti-spoofing, which has received little attention in the literature. Furthermore, it contains three visual modalities, *i.e.*, RGB, Depth, and IR. Summarizing, the main purpose of CASIA-CeFA is to provide with the largest up to date face anti-spoofing dataset to allow for the evaluation of the generalization performance of new PAD methods in three main aspects: cross-ethnicity, cross-modality and cross-attacks. In this section, we describe the CASIA-CeFA dataset in detail, including acquisition details, attack types, and proposed evaluation protocols.

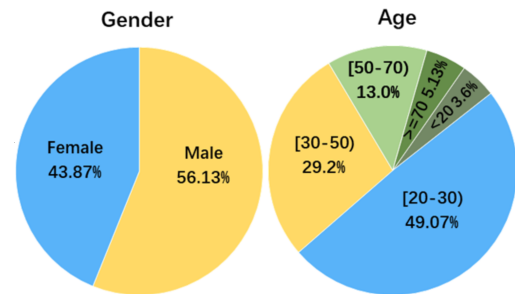


Figure 4. Age and gender distributions of the CASIA-CeFA.

**Acquisition Details.** We use the Intel Realsense to capture the RGB, Depth and IR videos simultaneously at 30

Prot.	Subset	Ethnicity			Subjects	Modalities			PAIs	# real videos	# fake videos	# all videos	
		1_1	1_2	1_3									
1	Train	A	C	E	1-200	R&D&I			Pr&Re	600/600/600	1800/1800/1800	2400/2400/2400	
	Valid	A	C	E	201-300	R&D&I			Pr&Re	300/300/300	900/900/900	1200/1200/1200	
	Test	C&E	A&E	A&C	301-500	R&D&I			Pr&Re	1200/1200/1200	6600/6600/6600	7800/7800/7800	
								2_1	2_2				
2	Train	A&C&E			1-200	R&D&I			Pr	Re	1800/1800	3600/1800	5400/3600
	Valid	A&C&E			201-300	R&D&I			Pr	Re	900/900	1800/900	2700/1800
	Test	A&C&E			301-500	R&D&I			Pe	Pr	1800/1800	4800/6600	6600/8400
					3_1	3_2	3_3						
3	Train	A&C&E			1-200	R	D	I	Pr&Re	600/600/600	1800/1800/1800	2400/2400/2400	
	Valid	A&C&E			201-300	R	D	I	Pr&Re	300/300/300	900/900/900	1200/1200/1200	
	Test	A&C&E			301-500	D&I	R&I	R&D	Pr&Re	1200/1200/1200	5600/5600/5600	6800/6800/6800	
		4_1	4_2	4_3									
4	Train	A	C	E	1-200	R	D	I	Re	600/600/600	600/600/600	1200/1200/1200	
	Valid	A	C	E	201-300	R	D	I	Re	300/300/300	300/300/300	600/600/600	
	Test	C&E	A&E	A&C	301-500	R	D	I	Pr	1200/1200/1200	5400/5400/5400	6600/6600/6600	

Table 2. Four evaluation protocols are defined for CASIA-CeFA; 1) cross-ethnicity, 2) cross-PAI, 3) cross-modality and 4) cross-ethnicity&PAI, respectively. Note that 3D attacks subset of CASIA-CeFA are included to the test set of every testing protocol (not shown in the table). R: RGB, D: Depth, I: IR, A: Africa, C: Central Asia, E: East Asia, Pr: print attack, Re: replay attack; & indicates merging; \*\_\* corresponds to the name of sub-protocols.

fps. The resolution is  $1280 \times 720$  pixels for each video frame and all modalities. Performers are asked to move smoothly their head so as to have a maximum of around  $30^\circ$  deviation of head pose in relation to frontal view. Data pre-processing is similar to the one performed in [41], expect that PRNet [13] is replaced by 3DFFA [44] for face region detection. Examples of original recorded images from video sequences and processed face regions for different visual modalities are shown in Fig. 1.

**Statistics.** As shown in Table 1, CASIA-CeFA consists of 2D and 3D attack subsets. For the 2D attack subset, it includes print and video-reply attacks, and three ethnicities (African, East Asian and Central Asian) with 2 attacks (print face from cloth and video-replay). Each ethnicity has 500 subjects. Each subject has 1 real sample, 2 fake samples of print attack captured in indoor and outdoor, and 1 fake sample of video-replay. In total, there are 18000 videos (6000 per modality). The age and gender statistics for the 2D attack subset of CASIA-CeFA is shown in Fig. 4.

For the 3D attack subset, it has 3D print mask and silica gel face attacks. For 3D print mask, it has 99 subjects, each subject with 18 fake samples captured in three attacks and six lighting environments. Attacks include only mask, wearing a wig and glasses, and wearing a wig and no glasses. Lighting conditions include outdoor sunshine, outdoor shade, indoor side light, indoor front light, indoor backlit and indoor regular light. In total, there are 5346 videos (1782 per modality). For silica gel face attacks, it has 8 subjects, each subject has 8 fake samples captured in two attacks styles and four lighting environments. Attacks include wearing a wig and glasses and wearing a wig and no glasses. Lighting environments include indoor side light, indoor front light, indoor backlit and indoor normal light. In total, there are 196 videos (64 per modality).

**Evaluation Protocols.** We design four protocols for the 2D attacks subset, as shown in Table 2, totalling 11 sub-protocols (1\_1, 1\_2, 1\_3, 2\_1, 2\_2, 3\_1, 3\_2, 3\_3, 4\_1, 4\_2, and 4\_3). We divide 500 subjects per ethnicity into three subject-disjoint subsets (second and fourth columns in Table 2). Each protocol has three data subsets: training, validation and testing sets, which contain 200, 100, and 200 subjects, respectively.

- **Protocol 1 (cross-ethnicity):** Most of the public face PAD datasets just contain a single ethnicity. Even though there are few datasets [20, 41] containing multiple ethnicities, they lack of ethnicity labels or do not provide with a protocol to perform cross-ethnicity evaluation. Therefore, we design the first protocol to evaluate the generalization of PAD methods for cross-ethnicity testing. One ethnicity is used for training and validation, and the left two ethnicities are used for testing. Therefore, there are three different evaluations (third column of Protocol 1 in Table 2).

- **Protocol 2 (cross-PAI):** Given the diversity and unpredictability of attack types from different presentation attack instruments (PAI), it is necessary to evaluate the robustness of face PAD algorithms to this kind of variations (sixth column of Protocol 2 in Table 2).

- **Protocol 3 (cross-modality):** Given the release of affordable devices capturing complementary visual modalities (*i.e.*, Intel Resense, Microsoft Kinect), recently the multi-modal face anti-spoofing dataset was proposed [41]. However, there is no standard protocol to explore the generalization of face PAD methods when different train-test modalities are considered for evaluation. We define three cross-modality evaluations, each of them having one modality for training and the two remaining ones for testing (fifth column of Protocol 3 in Table 2).

- **Protocol 4 (cross-ethnicity & PAI):** The most challeng-

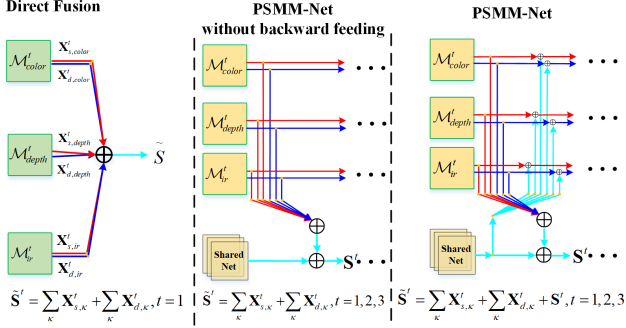


Figure 5. Comparison of network units for multi-modal fusion strategies. From left to right: NHF, PSMM-NET-WoBF and PSMM-Net. The fusion process for the  $t^{th}$  feature level of each strategy is shown at the bottom.

ing protocol is designed via combining the condition of both Protocol 1 and 2. As shown in Protocol 4 of Table. 2, the testing subset introduces two unknown target variations simultaneously.

Like [6], the mean and variance of evaluate metrics for these four protocols are calculated in our experiments. Detailed statistics for the different protocols are shown in Table 2. More information about CASIA-CeFA can be found in our supplementary material.

## 5. Experiments

In this section, we conduct a series of experiments on public available face anti-spoofing datasets to verify the effectiveness of our methodology and the benefits of the presented CASIA-CeFA dataset. In the following, we will introduce the employed datasets & metrics, implementation details, experimental setting, and results & analysis sequentially.

### 5.1. Datasets & Metrics

We evaluate the performance of PSMM-Net on two multi-modal (*i.e.*, RGB, Depth and IR) datasets: CASIA-CeFA and CASIA-SURF [41], while evaluate the SD-Net on two single-modal (*i.e.*, RGB) face anti-spoofing benchmarks: OULU-NPU [6] and SiW [20]. They are the mainstream datasets released in recent years with their own characteristics in terms of the number of subject, modality and ethnicity, attack types, acquisition device and PAIs *et al.*. Therefore, experiments on these datasets can verify the performance of our method more convincingly.

In order to perform a consistent evaluation with prior works, we report the experimental results using the following metrics based on respective official protocols: Attack Presentation Classification Error Rate (APCER) [1], Bona Fide Presentation Classification Error Rate (BPCER), Average Classification Error Rate (ACER), and Receiver Operating Characteristic (ROC) curve [41].

Prot. name	APCER(%)	BPCER(%)	ACER(%)	
Prot. 1	1_1	0.5	0.8	0.6
	1_2	4.8	4.0	4.4
	1_3	1.2	1.8	1.5
	Avg±Std	2.2±2.3	2.2±1.6	2.2±2.0
Prot. 2	2_1	0.1	0.7	0.4
	2_2	13.8	1.2	7.5
	Avg±Std	7.0±9.7	1.0±0.4	4.0±5.0
Prot. 3	3_1	8.9	0.9	4.9
	3_2	22.6	4.6	13.6
	3_3	21.1	2.3	11.7
	Avg±Std	17.5±7.5	2.6±1.9	10.1±4.6
Prot. 4	4_1	33.3	15.8	24.5
	4_2	78.2	8.3	43.2
	4_3	50.0	5.5	27.7
	Avg±Std	53.8±22.7	9.9±5.3	31.8±10.0

Table 3. PSMM-Net evaluation on the four protocols of CASIA-CeFA dataset, where A.B represents sub-protocol B from Protocol A, and Avg±Std indicates the mean and variance operation.

### 5.2. Implementation Details

The proposed PSMM-Net is implemented with TensorFlow [2] and run on a single NVIDIA TITAN X GPU. We resize the cropped face region to  $112 \times 112$ , and use random rotation within the range of  $[-180^0, 180^0]$ , flipping, cropping and color distortion for data augmentation. All models are trained for 25 epochs via Adaptive Moment Estimation (Adam) algorithm and initial learning rate of 0.1, which is decreased after 15 and 20 epochs with a factor of 10. The batch size of each CNN stream is 64, and the length of the consecutive frames used to construct dynamic map is set to 7 by our experimental experience. In addition, all fusion points in this work use element summation operations to prevent dimension explosion.

### 5.3. Baseline Model Evaluation

Before exploring the traits of our dataset, we first provide a benchmark for CASIA-CeFA based on the proposed method. From the Table 3, in which the results of the four protocols are derived from all the respective sub-protocols by calculating the mean and variance, we can draw the following conclusions: (1) from the results of the three sub-protocols in Protocol 1, the ACER scores are 0.6%, 4.4% and 1.5%, respectively, indicating that it is necessary to study the generalization of the face PAD method for different ethnicity; (2) In the case of Protocol 2, when print attack is used for training/validation and video-replay and 3D mask are used for testing, the ACER score is 0.4% (sub-protocol 2\_1), while video-replay attack is used for training/validation, and print attack and 3D attack are used for testing, with an ACER score of 7.5% (sub-protocol 2\_2). The large gap between the results of the two sub-protocols is mainly caused by different PAI (*i.e.*, different displays and

Prot.1	RGB			Depth			IR		
	APCER(%)	BPCER(%)	ACER(%)	APCER(%)	BPCER(%)	ACER(%)	APCER(%)	BPCER(%)	ACER(%)
S-Net	28.1±3.6	<b>6.4±4.6</b>	17.2±3.6	<b>5.6±3.0</b>	9.8±4.2	7.7±3.5	11.4±2.1	8.2±1.2	9.8±1.7
D-Net	20.6±4.0	19.3±9.0	19.9±4.0	11.2±5.1	7.5±1.5	9.4±2.0	8.1±1.8	14.4±3.8	11.3±2.1
SD-Net	<b>14.9±6.0</b>	10.3±1.8	<b>12.6±3.4</b>	7.0±8.1	<b>5.2±3.5</b>	<b>6.1±5.4</b>	<b>7.3±1.2</b>	<b>5.5±1.8</b>	<b>6.4±1.3</b>

Table 4. Ablation experiments on three single-modal groups: RGB, Depth and IR. Each modality group contains three experiments: static branch, dynamic branch and static-dynamic branch. Numbers in bold correspond to the best results per column.

Prot. name	RGB			Depth			IR		
	APCER(%)	BPCER(%)	(ACER%)	APCER(%)	BPCER(%)	(ACER%)	APCER(%)	BPCER(%)	(ACER%)
Prot. 1	14.9±6.0	10.3±1.8	12.6±3.4	7.0±8.1	5.2±3.5	6.1±5.4	7.3±1.2	5.5±1.8	6.4±1.3
Prot. 2	45.0±39.1	1.6±1.9	23.3±18.6	13.6±18.7	1.2±0.7	7.4±9.7	8.1±11.0	1.5±1.8	4.8±6.4
Prot. 3*	5.9	2.2	4.0	0.3	0.3	0.3	0.2	0.5	0.4
Prot. 4	65.8±16.4	8.3±6.5	35.2±5.8	18.5±8.2	7.0±5.2	12.7±5.7	6.8±2.9	4.2±3.3	5.5±2.2

Table 5. Experimental results of the SD-Net based on single modality on four protocols (\* indicates that the modal type of the testing subset is consistent with the training subset).

printers) create different artifacts. (3) Protocol 3 evaluates cross-modality. The best result is achieved for sub-protocol 3\_1, with ACER of 4.9%. The other two sub-protocols achieve a similar low performance score. This means the best performance is achieved when RGB data of 2D attack subset is used for training/validation while the other two modalities of 2D and 3D attack subsets are used for testing. (4) Protocol 4 is the most difficult evaluation scenario, which simultaneously considers cross-ethnicity and cross-PAI. All sub-protocols achieve poor performance, being 24.5%, 43.2%, and 27.7% ACER scores for 4\_1, 4\_2, and 4\_3 achieve, respectively.

#### 5.4. Ablation Analysis

In order to verify the effectiveness of the proposed method, we perform a series of ablation experiments on Protocol 1 (cross-ethnicity) of the CASIA-CeFA dataset.

**Static and Dynamic Features.** We evaluate S-Net (Static branch of SD-Net), D-Net (Dynamic branch of SD-Net) and SD-Net. Results for RGB, Depth and IR modalities are shown in Table 4. Compared with S-Net and D-Net, SD-Net achieves superior performance. For RGB, Depth and IR modalities, ACER of SD-Net is 12.6%, 6.1%, 6.4%, versus 17.2%, 7.7%, 9.4% of S-Net (improved by 4.6%, 1.6%, 3.4%) and 19.9%, 9.4%, 11.3% of D-Net (improved by 7.3%, 3.3%, 4.9%), respectively. Furthermore, Table 4 shows that the performance of Depth and IR modalities are superior to the one of RGB. One reason is the variability in lighting conditions included in CASIA-CeFA.

In addition, we provide the results of single-modal experiments on the 4 protocols to facilitate comparison of face PAD algorithms, shown in Table 5. It shows that when only single modality is used, the performance of the depth or IR modality is superior to that of the RGB modality.

**Multiple Modalities.** In order to show the effect of analysing a different number of modalities, we evaluate one modality (RGB), two modalities (RGB and Depth), and

Prot.1	PSMM-Net		
	APCER(%)	BPCER(%)	ACER(%)
RGB	14.9±6.0	10.3±1.8	12.6±3.4
RGB&Depth	2.3±2.9	9.2±5.9	5.7±3.5
RGB&Depth&IR	<b>2.2±2.3</b>	<b>2.2±1.6</b>	<b>2.2±2.0</b>

Table 6. Ablation experiments on the effect of multiple modalities. Numbers in bold correspond to the best result per column.

Method	APCER(%)	BPCER(%)	ACER(%)
NHF	25.3±12.2	4.4±3.1	14.8±6.8
PSMM-WoBF	12.7±0.4	3.2±2.3	7.9±1.3
PSMM-Net	<b>2.2±2.3</b>	<b>2.2±1.6</b>	<b>2.2±2.0</b>

Table 7. Comparison of fusion strategies in Protocol 1 of CASIA-CeFA. The number in black indicates best results.

three modalities (RGB, Depth and IR) on PSMM-Net. As shown in Fig. 3, the PSMM-Net contains three SD-Nets and one shared branch. When only RGB modality is considered, we just use one SD-Net for evaluation. When two or three modalities are considered, we use two or three SD-Nets and one shared branch to train the PSMM-Net model, respectively. Results are shown in Table 6. The best results are obtained when using all three modalities, which 2.2% of APCER, 2.2% of BPCER and 2.2% of ACER. Compared with the performance of using single RGB modality and two modalities, the improvement in performance corresponds to 12.7% and 0.1% for APCER, 8.1% and 7.2% for BPCER, and 10.4% and 3.5% for ACER, respectively.

**Fusion Strategy.** In order to evaluate the performance of PSMM-Net, we compare it with other two variants: Naive halfway fusion (NHF) and PSMM-Net without backward feeding mechanism (PSMM-Net-WoBF). As shown in Fig. 5, NHF combines the modules of different modalities at a later stage (*i.e.*, after  $\mathcal{M}_r^1$  module) and PSMM-Net-WoBF strategy removes the backward feeding from PSMM-Net. The fusion comparison results are shown in Table 7, showing higher performance of the proposed PSMM-Net, with

Method	TPR (%)			APCER (%)	BPCER (%)	ACER (%)
	@FPR=10 <sup>-2</sup>	@FPR=10 <sup>-3</sup>	@FPR=10 <sup>-4</sup>			
NHF fusion [41]	89.1	33.6	17.8	5.6	3.8	4.7
Single-scale SE fusion [41]	96.7	81.8	56.8	3.8	1.0	2.4
Multi-scale SE fusion [40]	99.8	98.4	95.2	1.6	0.08	0.8
PSMM-Net	<b>99.9</b>	99.3	96.2	0.7	0.06	0.4
PSMM-Net(CASIA-CeFA)	<b>99.9</b>	<b>99.7</b>	<b>97.6</b>	<b>0.5</b>	<b>0.02</b>	<b>0.2</b>

Table 8. Comparison of the proposed method with three fusion strategies. All models are trained on the CASIA-SURF training subset and tested on the testing subset. Best results are bolded.

ACER of 2.2%.

## 5.5. Methods Comparison

**CASIA-SURF Dataset.** Comparison results are shown in Table 8. The performance of the PSMM-Net is superior to the ones of the competing multi-modal fusion methods, including Halfway fusion [41], single-scale SE fusion [41], and multi-scale SE fusion [40]. When compared with [41, 40], PSMM-Net improves the performance by at least 0.9% for APCER, 0.02% for NPECE, and 0.4% for ACER. When the PSMM-Net is pretrained on CASIA-CeFA, it further improves performance. Concretely, the performance of  $TPR@FPR = 10^{-4}$  is increased by 2.4% when pretraining with the proposed CASIA-CeFA dataset.

In 2019 a challenge on the CASIA-SURF dataset was run at CVPR<sup>1</sup>. The results of the challenge were very promising, where 3 winning teams VisionLab [25], ReadSense [29] and Feather [39] got  $TPR=99.87\%@FPR = 10^{-4}$ ,  $99.81\%@FPR = 10^{-4}$  and  $99.14\%@FPR = 10^{-4}$ , respectively. The 2 main reasons of these high performance are: 1) *several external datasets were used*. VisionLab [25] used four large-scale datasets, namely CASIA-WebFace [38], MSCeleb-1M [15], AFAD-lite [23] and Asian dataset [43] for pretraining, while Feather [39] used a large private dataset with a collection protocol similar to CASIA-SURF. 2) *Many network ensembles*. VisionLab [25], ReadSense [29], and Feather [39] average the outputs of 24, 12 and 10 networks to compute final results. Thus in order to have a fair comparison we omit VisionLab [25], ReadSense [29] and Feather [39] from Table 8.

**SiW Dataset.** Results for this dataset are shown in Table 9. We compare the proposed SD-Net with other methods without pretraining. Taking the Protocol 1 of SiW as an example, SD-Net achieves the best ACER of 0.74%, an improvement of 0.26% with respect to the second best score, 1.00% (ACER) from STASN [37]. In terms of CASIA-CeFA pretraining, our method is competitive to STASN (Data) [37] (0.35% versus 0.3% in term of ACER), which used an large private dataset as pretrain. For Protocol 2 and 3 of SiW, our methods has achieved the best performance under three evaluation metrics.

<sup>1</sup><https://sites.google.com/qq.com/chalearnfacespoofingattackdete/welcome>

Prot.	Method	APCER (%)	BPCER (%)	ACER (%)	Pretrain
1	FAS-BAS [20]	3.58	3.58	3.58	No
	FAS-TD-SF [34]	1.27	<b>0.83</b>	1.05	
	STASN [37]	-	-	1.00	
	SD-Net	<b>0.14</b>	1.34	<b>0.74</b>	
	FAS-TD-SF (CASIA-SURF) [41]	1.27	<b>0.33</b>	0.80	Yes
	STASN (Data) [37]	-	-	<b>0.30</b>	
SD-Net (CASIA-CeFA)	<b>0.21</b>	0.50	0.35		
2	FAS-BAS [20]	0.57±0.69	0.57±0.69	0.57±0.69	No
	FAS-TD-SF [34]	0.33±0.27	<b>0.29±0.39</b>	0.31±0.28	
	STASN [37]	-	-	0.28±0.05	
	SD-Net	<b>0.25±0.32</b>	<b>0.29±0.34</b>	<b>0.27±0.28</b>	
	FAS-TD-SF (CASIA-SURF) [41]	<b>0.08±0.17</b>	0.25±0.22	0.17±0.16	Yes
	STASN (Data) [37]	-	-	<b>0.15±0.05</b>	
SD-Net (CASIA-CeFA)	0.09±0.17	<b>0.21±0.25</b>	<b>0.15±0.11</b>		
3	FAS-BAS [20]	8.31±3.81	8.31±3.81	8.31±3.81	No
	FAS-TD-SF [34]	7.70±3.88	<b>7.76±4.09</b>	7.73±3.99	
	STASN [37]	-	-	12.10±1.50	
	SD-Net	<b>3.74±2.15</b>	7.85±1.42	<b>5.80±0.36</b>	
	FAS-TD-SF (CASIA-SURF) [41]	6.27±4.36	<b>6.43±4.42</b>	6.35±4.39	Yes
	STASN (Data) [37]	-	-	5.85±0.85	
SD-Net (CASIA-CeFA)	<b>2.70±1.56</b>	7.10±1.56	<b>4.90±0.00</b>		

Table 9. Comparisons on SiW. '-' indicates unprovided; '( )' means the method is used a pretrain model trained from a specific dataset. Best results are bolded in the condition of with/without pretrain.

Prot.	Method	APCER (%)	BPCER (%)	ACER (%)	Pretrain
3	FAS-BAS [20]	<b>2.7±1.3</b>	3.1±1.7	2.9±1.5	No
	FAS-Ds [17]	4.0±1.8	3.8±1.2	3.6±1.6	
	STASN [37]	4.7±3.9	0.9±1.2	2.8±1.6	
	SD-Net	<b>2.7±2.5</b>	<b>1.4±2.0</b>	<b>2.1±1.4</b>	
	STASN (Data) [37]	<b>1.4±1.4</b>	3.6±4.6	2.5±2.2	Yes
	SD-Net (CASIA-CeFA)	2.7±2.5	<b>0.9±0.9</b>	<b>1.8±1.4</b>	
4	FAS-BAS [20]	9.3±5.6	10.4±6.0	9.5±6.0	No
	FAS-Ds [17]	5.1±6.3	<b>6.1±5.1</b>	5.6±5.7	
	STASN [37]	6.7±10.6	8.3±8.4	7.5±4.7	
	SD-Net	<b>4.6±5.1</b>	6.3±6.3	<b>5.4±2.8</b>	
	STASN (Data) [37]	<b>0.9±1.8</b>	<b>4.2±5.3</b>	<b>2.6±2.8</b>	Yes
	SD-Net (CASIA-CeFA)	5.0±4.7	4.6±4.6	4.8±2.7	

Table 10. Results of Protocol 3 and 4 on OULU-NPU. '( )' means the method is used a pretrain model trained from a specific dataset. Best results are bolded in the conditions of with/without pretrain.

**OULU-NPU Dataset.** We perform evaluation on the 2 most challenging protocols of OULU-NPU. Protocol 3 studies the generalization across different acquisition devices and Protocol 4 considers all the conditions of previous three protocols simultaneously. The experimental Results are shown in Table 10. In the case of comparison without pretraining, SD-Net obtains the best results in both Pro-

TOCOL 3 and 4. The ACER of our SD-Net is 2.1% versus 2.8% of STASN [37]. When comparing the results using pretraining, our method achieves the first and second position for Protocol 3 and 4, respectively. Based on the above experiments, when without using pretraining, the proposed method can get the state-of-the-art performance (ACER) in all protocols on SiW and OULU-NPU. The proposed method with pretraining on CASIA-CeFA can also get the best ACER scores on most of protocols. Those experimental results clearly demonstrate the effectiveness of the proposed method and the collected CASIA-CeFA dataset.

## 6. Conclusion

In this paper, we have presented the CASIA-CeFA dataset for face anti-spoofing. This corresponds to the largest public available dataset in terms of modalities, subjects, ethnicities and attacks. Moreover, we have proposed a static- and dynamic- network (SD-Net) to learn both static and dynamic features from single-modal. Then, we have proposed a partially shared multi-modal network (PSMM-Net) to learn complementary information from multi-modal data in videos. Extensive experiments on four popular datasets show the high generalization capability of the proposed SD-Net and PSMM-Net, and the utility and challenges of the released CASIA-CeFA dataset.

## References

- [1] ISO/IEC JTC 1/SC 37 Biometrics. information technology biometric presentation attack detection part 1: Framework. international organization for standardization. 2016. <https://www.iso.org/obp/ui/iso>.
- [2] Martn Abadi, Paul Barham, Jianmin Chen, Zhifeng Chen, Andy Davis, Jeffrey Dean, Matthieu Devin, Sanjay Ghemawat, Geoffrey Irving, and Michael Isard. Tensorflow: A system for large-scale machine learning.
- [3] Yousef Atoum, Yaojie Liu, Amin Jourabloo, and Xiaoming Liu. Face anti-spoofing using patch and depth-based cnns. In *IJCB*, pages 319–328. IEEE, 2017.
- [4] Zinelabidine Boulkenafet, Jukka Komulainen, and Abdenour Hadid. Face spoofing detection using colour texture analysis. *TIFS*, 2016.
- [5] Zinelabidine Boulkenafet, Jukka Komulainen, and Abdenour Hadid. Face antispoofing using speeded-up robust features and fisher vector encoding. *SPL*, 2017.
- [6] Zinelabinde Boulkenafet, Jukka Komulainen, Lei Li, Xiaoyi Feng, and Abdenour Hadid. Oulu-npu: A mobile face presentation attack database with real-world variations. In *FG*, 2017.
- [7] I. Chingovska, A. Anjos, and S. Marcel. On the effectiveness of local binary patterns in face anti-spoofing. In *Biometrics Special Interest Group*, 2012.
- [8] Ivana Chingovska, Nesli Erdogmus, André Anjos, and Sébastien Marcel. Face recognition systems under spoofing attacks. In *Face Recognition Across the Imaging Spectrum*. 2016.
- [9] Artur Costa-Pazo, Sushil Bhattacharjee, Esteban Vazquez-Fernandez, and Sebastien Marcel. The replay-mobile face presentation-attack database. In *BIO SIG*, 2016.
- [10] Tiago de Freitas Pereira, André Anjos, José Mario De Martino, and Sébastien Marcel. Can face anti-spoofing countermeasures work in a real world scenario? In *ICB*, 2013.
- [11] Nesli Erdogmus and Sebastien Marcel. Spoofing in 2d face recognition with 3d masks and anti-spoofing with kinect. In *BTAS*, 2014.
- [12] Litong Feng, Lai-Man Po, Yuming Li, Xuyuan Xu, Fang Yuan, Terence Chun-Ho Cheung, and Kwok-Wai Cheung. Integration of image quality and motion cues for face anti-spoofing: A neural network approach. *JVCIR*, 2016.
- [13] Yao Feng, Fan Wu, Xiaohu Shao, Yanfeng Wang, and Xi Zhou. Joint 3d face reconstruction and dense alignment with position map regression network. In *ECCV*, 2018.
- [14] Basura Fernando, Efstratios Gavves, José Oramas, Amir Ghodrati, and Tinne Tuytelaars. Rank pooling for action recognition. *TPAMI*, 39(4):773–787, 2017.
- [15] Yandong Guo, Lei Zhang, Yuxiao Hu, Xiaodong He, and Jianfeng Gao. Ms-celeb-1m: A dataset and benchmark for large-scale face recognition. In *ECCV*, pages 87–102. Springer, 2016.
- [16] Kaiming He, Xiangyu Zhang, Shaoqing Ren, and Jian Sun. Deep residual learning for image recognition. In *CVPR*, 2016.
- [17] Amin Jourabloo, Yaojie Liu, and Xiaoming Liu. Face de-spoofing: Anti-spoofing via noise modeling. *arXiv*, 2018.
- [18] Jukka Komulainen, Abdenour Hadid, and Matti Pietikainen. Context based face anti-spoofing. In *BTAS*, 2013.
- [19] Lei Li, Xiaoyi Feng, Zinelabidine Boulkenafet, Zhaoqiang Xia, Mingming Li, and Abdenour Hadid. An original face anti-spoofing approach using partial convolutional neural network. In *IPTA*, 2016.
- [20] Yaojie Liu, Amin Jourabloo, and Xiaoming Liu. Learning deep models for face anti-spoofing: Binary or auxiliary supervision. In *CVPR*, 2018.
- [21] Yaojie Liu, Joel Stehouwer, Amin Jourabloo, and Xiaoming Liu. Deep tree learning for zero-shot face anti-spoofing. In *CVPR*, pages 4680–4689, 2019.
- [22] Jukka Määttä, Abdenour Hadid, and Matti Pietikainen. Face spoofing detection from single images using micro-texture analysis. In *IJCB*, pages 1–7. IEEE, 2011.
- [23] Zhenxing Niu, Mo Zhou, Le Wang, Xinbo Gao, and Gang Hua. Ordinal regression with multiple output cnn for age estimation. In *CVPR*, pages 4920–4928, 2016.
- [24] Gang Pan, Lin Sun, Zhaohui Wu, and Shihong Lao. Eyeblink-based anti-spoofing in face recognition from a generic webcam. In *ICCV*, 2007.
- [25] Aleksandr Parkin and Oleg Grinchuk. Recognizing multi-modal face spoofing with face recognition networks. In *PRCVW*, pages 0–0, 2019.
- [26] Keyurkumar Patel, Hu Han, and Anil K Jain. Cross-database face antispoofing with robust feature representation. In *CCBR*, 2016.
- [27] Keyurkumar Patel, Hu Han, and Anil K Jain. Secure face unlock: Spoof detection on smartphones. *TIFS*, 2016.

- [28] Rui Shao, Xiangyuan Lan, Jiawei Li, and Pong C Yuen. Multi-adversarial discriminative deep domain generalization for face presentation attack detection. In *CVPR*, pages 10023–10031, 2019.
- [29] Tao Shen, Yuyu Huang, and Zhijun Tong. Facebagnet: Bag-of-local-features model for multi-modal face anti-spoofing. In *PRCVW*, pages 0–0, 2019.
- [30] Alex J Smola and Bernhard Schölkopf. A tutorial on support vector regression. *Statistics and computing*, 14(3):199–222, 2004.
- [31] Zichang Tan, Yang Yang, Jun Wan, Guodong Guo, and Stan Li. Deeply-learned hybrid representations for facial age estimation. pages 3548–3554, 08 2019.
- [32] Jue Wang, Anoop Cherian, and Fatih Porikli. Ordered pooling of optical flow sequences for action recognition. In *WACV*, pages 168–176. IEEE, 2017.
- [33] Pichao Wang, Wanqing Li, Jun Wan, Philip Ogunbona, and Xinwang Liu. Cooperative training of deep aggregation networks for rgb-d action recognition. In *Thirty-Second AAAI Conference on Artificial Intelligence*, 2018.
- [34] Zezheng Wang, Chenxu Zhao, Yunxiao Qin, Qiusheng Zhou, and Zhen Lei. Exploiting temporal and depth information for multi-frame face anti-spoofing. *arXiv*, 2018.
- [35] Di Wen, Hu Han, and Anil K Jain. Face spoof detection with image distortion analysis. *TIFS*, 2015.
- [36] Jianwei Yang, Zhen Lei, Shengcai Liao, and Stan Z Li. Face liveness detection with component dependent descriptor. In *ICB*, 2013.
- [37] Xiao Yang, Wenhan Luo, Linchao Bao, Yuan Gao, Dihong Gong, Shibao Zheng, Zhifeng Li, and Wei Liu. Face anti-spoofing: Model matters, so does data. In *CVPR*, pages 3507–3516, 2019.
- [38] Dong Yi, Zhen Lei, Shengcai Liao, and Stan Z Li. Learning face representation from scratch. *arXiv*, 2014.
- [39] Peng Zhang, Fuhao Zou, Zhiwen Wu, Nengli Dai, Skarpness Mark, Michael Fu, Juan Zhao, and Kai Li. Feathernets: Convolutional neural networks as light as feather for face anti-spoofing. 2019.
- [40] Shifeng Zhang, Ajian Liu, Jun Wan, Yanyan Liang, Guogong Guo, Sergio Escalera, Hugo Jair Escalante, and Stan Z Li. Casia-surf: A large-scale multi-modal benchmark for face anti-spoofing. *arXiv:1908.10654*, 2019.
- [41] Shifeng Zhang, Xiaobo Wang, Ajian Liu, Chenxu Zhao, Jun Wan, Sergio Escalera, Hailin Shi, Zezheng Wang, and Stan Z. Li. A dataset and benchmark for large-scale multi-modal face anti-spoofing. In *CVPR*, 2019.
- [42] Zhiwei Zhang, Junjie Yan, Sifei Liu, Zhen Lei, Dong Yi, and Stan Z Li. A face antispoofing database with diverse attacks. In *ICB*, 2012.
- [43] Jian Zhao, Yu Cheng, Yan Xu, Lin Xiong, Jianshu Li, Fang Zhao, Karlekar Jayashree, Sugiri Pranata, Shengmei Shen, Junliang Xing, et al. Towards pose invariant face recognition in the wild. In *CVPR*, pages 2207–2216, 2018.
- [44] Xiangyu Zhu, Xiaoming Liu, Zhen Lei, and Stan Z Li. Face alignment in full pose range: A 3d total solution. *TPAMI*, 41(1):78–92, 2017.